A new instability in laser produced plasmas

Contact j.bissell07@imperial.ac.uk

J. J. Bissell, C. P. Ridgers and R. J. Kingham

Blackett Laboratory, Imperial College of Science, Technology and Medicine, London SW7 2BZ, UK

Abstract

The mechanism for a new instability is discussed and a dispersion relation derived. Unstable behaviour is shown to result from feedback between the Nernst Effect and the Righi-Leduc heat-flow. Calculations based on the parameters used in a recent nanosecond laser gas-jet experiment [1] predict growth of perturbations with typical wavelengths of order 50 μm and characteristic growth times of 0.15 ns. The distortion of both magnetic field and temperature profiles by the instability acts to concentrate heat-flow into 'islands' and may have implications for plasmas in which a high degree of symmetry is important.

Introduction

The existence of large self-generated magnetic fields (~100 T) in laser-produced plasmas [2] has long been known, and in recent years several experiments have been designed to assess their impact on inertial confinement fusion (I.C.F.) schemes [3] and to study more general magnetic phenomena in laser plasmas, such as magnetic reconnection [4] and instability [5]. In addition, there has been increased discussion of the possible uses for applied magnetic fields – for example, in the suppression of non-local transport (1) and the control of plasma density channels [6].

In this article we report a new instability that leads to disruption of magnetic field and thermal energy distributions, and results in the formation of large heat-flow 'islands'. For these reasons it is likely to have an impact on plasmas in which either self-generated or applied magnetic fields are present.

In our case unstable behaviour is driven purely by transport processes, specifically the interaction of the Nernst effect and the Righi-Leduc heat flow, and does not require hydrodynamic motion. In addition, positive feedback acts on existing magnetic fields (the process does not itself generate field) and is exhibited even when there are no gradients in electron number density. Furthermore, the terms responsible for growth go as $k^{3/2}$, where k is the wavenumber of an unstable perturbation, rather than the more usual k^2. In these ways what we see is distinct from instabilities existing in the literature, such as those of Tidman-Shanny [7,8], Weibal [9] and others [10,11,12].

For current purposes, and so that the relevance of the instability may be made more clear, we focus on an applied field case, specifically the geometry of Froula *et al*. (2007) – in simulations of which the instability

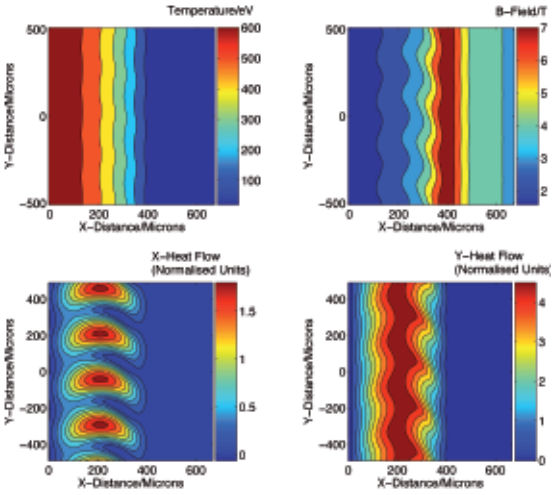

Figure 1. A snapshot of the instability from simulations using the kinetic code IMPACT and taken from [8]. The plasma was initially magnetised by a uniform field of 4 T, nevertheless, by the time of this snapshot (885 ps) much of the field has been wafted away from the line $x = 0$ by Nernst advection parallel to the x-axis (top right). Bulk temperature gradients in the x-direction and heat-flow islands are illustrated in the contour projections at the top and bottom left respectively. Notice the large heat-flow in the y-direction caused primarily by the Righi-Leduc effect (bottom right).

was first observed [13]. In this experiment a nitrogen gas-jet (atomic number $Z = 7$) with electron number density $n_e = 1.5 \times 10^{-19}$ cm^{-3} and initial temperature $T_e = 20$ eV was subject to inverse bremsstrahlung heating for 1ns by a long-pulse laser of wavelength 1.045 μm and intensity 6.3×10^{14} Wcm^{-2}. Uniform magnetic fields of strengths up to 12 T were imposed parallel to the laser-heating beam and the radial heat-flow q_r inferred.

Like Froula *et al*., we focus on a two-dimensional cross-section through a plasma perpendicular to applied magnetic fields and the laser-heating beam. However, for ease of analysis we consider an x-y, rather than r-θ geometry, with a laser-heating strip in the y-direction instead of a circular laser spot [14]. In this way, the principle plasma temperature gradients and Nernst velocities are parallel to the x-axis of the system (see figure 1).

Modeling the system

Our discussion revolves around two key transport processes in magnetised plasmas: the Nernst effect, which results in advection of magnetic fields with heat-flux[15]; and the Righi-Leduc heat-flow[16], which describes the 'bending' of the heat-flow by magnetic fields acting on negatively charged heat-carrying electrons. Both phenomena are partly illustrated in figure 1.

The bulk evolution of the plasma temperature, by laser-heating, and magnetic field, by the Nernst effect, complicates any attempt at a perturbation analysis of the instability. However, progress can be made by contriving a steady-state.

Suppose a plasma exhibited magnetic field and temperature profiles as though it had been heated (such profiles may be obtained from stable heating runs); by 'turning-off' relevant physics one could, providing there were no further heating, construct an arrangement with temperature and magnetic field gradients that was also non-evolving. This has been our approach and has allowed us to study unstable behaviour by perturbing a somewhat artificial system.

Equation set

If we neglect hydrodynamic motion and take $\nabla n_e = 0$, the relevant physics may be described by the magnetic field induction equation, the electron thermal-energy continuity equation and the equations of classical transport (Braginskii's transport equations). The necessarily neglected terms are those parts of the thermal conductivity, electrical resistivity and the Nernst and Ettingshausen terms that lead to evolution of the plasma in the x-direction. In this way the equations governing the instability become:

$$\frac{\partial \mathbf{B}}{\partial t} = -\nabla\times\mathbf{E} = -\nabla\times\left(\frac{m_e}{e^2 n_e \tau_B \mu_0}\underline{\underline{\alpha}}\cdot\nabla\times\mathbf{B}\right) + \frac{1}{e}\nabla\times\left(\underline{\underline{\beta}}\cdot\nabla T_e\right) \quad (1)$$

and

$$\frac{\partial T_e}{\partial t} = -\frac{2}{3n_e}\nabla\cdot\mathbf{q}_T = \frac{2}{3}\nabla\cdot\left(\frac{\tau_B T_e}{m_e}\underline{\underline{\kappa}}\cdot\nabla T_e\right) + \frac{2}{3}\nabla\cdot\left(\frac{T_e}{en_e\mu_0}\underline{\underline{\psi'}}\cdot\nabla\times\mathbf{B}\right), \quad (2)$$

where we have substituted for the current using Ampère's Law

$$\mathbf{j} = \frac{1}{\mu_0}\nabla\times\mathbf{B}, \quad (3)$$

and neglected both Ohmic heating in the energy equation and convection by electron motion in the induction equation. The transport terms in equations (1) and (2), after neglecting the appropriate physics, take the form

$$\underline{\underline{\alpha}}\cdot\nabla\times\mathbf{B} = -\alpha_\perp\frac{\partial B}{\partial y}\mathbf{x}, \quad (4)$$

$$\underline{\underline{\beta}}\cdot\nabla T_e = -\beta_\wedge\frac{\partial T_e}{\partial y}\mathbf{x}, \quad (5)$$

$$\underline{\underline{\kappa}}\cdot\nabla T_e = \kappa_\perp\frac{\partial T_e}{\partial y} + \kappa_\wedge\mathbf{b}\times\nabla T_e, \quad (6)$$

and

$$\underline{\underline{\psi'}}\cdot\nabla\times\mathbf{B} = \psi'_\perp\nabla\times\mathbf{B} + \psi'_\wedge\frac{\partial B}{\partial x}\mathbf{y}, \quad (7)$$

where $\mathbf{B} = B\mathbf{b}$ defines a unit vector $\mathbf{b}$ in the direction of the magnetic field ($B = |\mathbf{B}|$) and $\mathbf{x}$ and $\mathbf{y}$ are unit vectors in the x and y directions. The coefficient ψ' is used to account for the full heat-flow $\mathbf{q}_T = \mathbf{q}_e - (5T_e/2e)\mathbf{j}$, where $\mathbf{q}_e$ is the electron intrinsic heat-flow[17], so that $\psi'_\perp = \beta_\perp + 5/2$ and $\beta_\wedge = \psi'_\wedge$. Care must be taken to employ the Braginskii collision time τ_B rather than the thermal collision time[18] $\tau = (2T_e/m_e)^{1/2} = (4/3\pi^{1/2})\tau_B$. The dimensionless transport coefficients $\alpha_\perp$, $\beta_\wedge$, $\kappa_\perp$, $\kappa_\wedge$, $\psi'_\perp$ and $\psi'_\wedge$ are calculated using polynomial fits[19,20], and are functions of the Hall parameter $\chi = \omega_e\tau_B$ only - where $\omega_e = eB/m_e$ is the electron gyro-frequency. The Nernst effect and the Righi-Leduc heat-flow, are described by terms in $\beta_\wedge$ and $\kappa_\wedge$ respectively. [Note: we have neglected the coefficients $\alpha_\wedge$ and $\beta_\perp$ which yield only small corrections.]

Perturbation analysis

The unperturbed plasma is given temperature and magnetic field profiles, T_0 and $\mathbf{B}_0 = B_0\mathbf{b}$ respectively, in the x-direction (no gradients in the y-direction) as calculated from 1-D linear heating simulations of Froula's experiment (see figure 2).

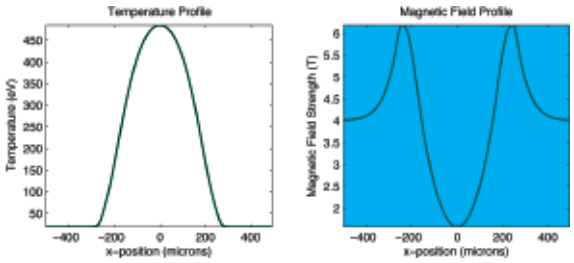

Figure 2. Temperature and magnetic field profiles at 500 ps used in the steady state model. These snapshots are taken from a 1-D linear simulation of the experiment of Froula *et al.* using the extended transport code Code_29 for the case of a 4 T applied field.

These background profiles are found to be static, i.e. $\partial T_0/\partial t = \partial B_0/\partial t = 0$, where, since it is always in the z-direction, we have expressed the magnetic field in scalar form. For our stability analysis we add wavelike perturbations in the y-direction to these background profiles such that

$$T_e = T_0(x) + \delta T(y,t) \qquad (\delta T = \delta T' \exp i(ky - \omega t)) \quad (8)$$

and

$$B = B_0(x) + \delta B(y,t) \qquad (\delta B = \delta B' \exp i(ky - \omega t)), \quad (9)$$

where k is the perturbation wavenumber, ω the frequency and δT' and δB' are phasors. Substitution of equations (8) and (9) into (1) and (2) yield to first order

$$\omega = -ik^2\left(\frac{m_e\alpha_\perp}{e^2 n_e\tau_B\mu_0} + \frac{\beta_\wedge}{e}\frac{\delta T}{\delta B}\right) \quad (10)$$

and

$$\omega = -\frac{2}{3}k\left(\frac{\tau_B T_0}{m_e}\frac{\partial\kappa_\wedge}{\partial\chi}\frac{e\tau_B}{m_e} + \frac{1}{en_e\mu_0}\left[\psi'_\perp + \frac{3}{2}\chi\frac{\partial\psi'_\perp}{\partial\chi}\right]\right)\left(\frac{\delta B}{\delta T}\frac{\partial T_0}{\partial x} - \frac{\partial B_0}{\partial x}\right) \quad (11)$$
$$-\frac{2}{3}ik^2\left(\frac{\tau_B T_0\kappa_\perp}{m_e} + \frac{\psi'_\wedge T_0}{en_e\mu_0}\frac{\delta B}{\delta T}\right)$$

respectively, where in deriving (10) and (11), we have used the results

$$\left|\frac{\chi}{\psi'_{\wedge}}\frac{\partial\psi'_{\wedge}}{\partial\chi}\right| = \left|\frac{\chi}{\beta_{\wedge}}\frac{\partial\beta_{\wedge}}{\partial\chi}\right| \sim \left|\frac{\chi}{\kappa_{\perp}}\frac{\partial\kappa_{\perp}}{\partial\chi} + 1\right| \le 1, \tag{12}$$

$$0 < \frac{\chi}{\alpha_{\perp}}\frac{\partial\alpha_{\perp}}{\partial\chi} < \frac{1}{4} \quad \text{and} \quad \frac{\delta T}{T_0} \sim \frac{\delta B}{B_0} << 1. \tag{13}$$

Eliminating $\delta T/\delta B$ from equations (10) and (11), and by using the definitions

$$a_1 = \frac{\beta_{\wedge}}{e}, \qquad a_2 = \frac{\alpha_{\perp} m_e}{e^2 n_e \tau_B \mu_0}, \tag{14}$$

$$b_1 = \frac{2}{3}\left(\frac{\tau_B T_0}{m_e}\frac{\partial\kappa_{\wedge}}{\partial\chi}\frac{e\tau_B}{m_e} + \frac{1}{en_e\mu_0}\left[\psi'_{\perp} + \frac{3}{2}\chi\frac{\partial\psi'_{\perp}}{\partial\chi}\right]\right)\frac{\partial T_0}{\partial x}, \tag{15}$$

$$b_2 = \frac{2}{3}\left(\frac{\tau_B T_0}{m_e}\frac{\partial\kappa_{\wedge}}{\partial\chi}\frac{e\tau_B}{m_e} + \frac{1}{en_e\mu_0}\left[\psi'_{\perp} + \frac{3}{2}\chi\frac{\partial\psi'_{\perp}}{\partial\chi}\right]\right)\frac{\partial B_0}{\partial x}, \tag{16}$$

$$b_3 = \frac{2}{3}\frac{\tau_B T_0 \kappa_{\perp}}{m_e}, \quad \text{and} \quad b_4 = \frac{2\psi'_{\wedge} T_0}{3 en_e\mu_0} \tag{17}$$

we obtain the dispersion relation for these wavelike perturbations:

$$\omega = b_2 k - (a_2 + b_3)ik^2 \pm \left[(b_2 k - (a_2 + b_3)ik^2)^2 + 4(a_1 b_1 + a_2 b_2)ik^3 + 4(a_2 b_3 - a_1 b_4)k^4\right]^{\frac{1}{2}}. \tag{18}$$

The positive root of this equation is unstable for a range of k up to a cut-off and predicts a growth rate equal to the imaginary part of ω (see figure 3).

Equations (15) and (16), with their dependence on the background temperature and magnetic field profiles, indicate that for realistic scenarios the unstable behavior will vary both temporally, as $\partial T_0/\partial x$ and $\partial B_0/\partial x$ evolve in time, and spatially, since the gradients are a function of position. For this reason theoretical predictions of the growth of the instability are limited to a particular cross-section in x and based on a given snapshot of the bulk profile.

Unstable behaviour is driven primarily by feedback between the Nernst effect and the Righi-Leduc heat-flow – phenomena accounted for by the $\beta_{\wedge}$ and $\kappa_{\wedge}$ contribution to the term $a_1 b_1$ in the dispersion relation. Notice that this results in growth that goes as $k^{3/2}$, while the most important damping effects, namely thermal and resistive diffusion, are proportional to k^2. Broadly speaking it is this that gives us the range of k for unstable behaviour and the shape of the dispersion curve in figure 3 ($\forall c_1, c_2 \in \mathbb{R}^+$, $\forall k \in \mathbb{R}^+$ such that $c_1 k^{3/2} - c_2 k^2 > 0$).

The fastest growing perturbation for the conditions described in figure 3 has a wavenumber of approximately 0.007 (normalised units), corresponding to a wavelength of $\lambda \approx 50$ μm. At this wavelength the growth rate is about 0.00015 (normalised units) or $\omega_{max} \approx 7$ Ghz yielding a characteristic growth time $t_{char} = 1/\omega_{max} \approx 0.15$ ns. Figure 3 indicates reasonable agreement between theory and simulation given the somewhat crude nature of our approximations.

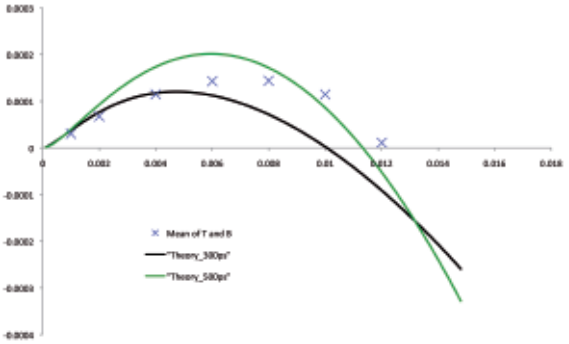

Figure 3. The theoretical dispersion relation for a cross-section at $x \approx 100$ μm from snapshots taken at 300 ps (black curve) and 500 ps (green curve). The x-axis represents the wavenumber normalised to $\approx 5.6 \times 10^{-8}$ m and the y-axis the perturbation growth rate normalised to $\approx 2.2 \times 10^{-14}$ s. Blue crosses are growth rates measured from simulations of a plasma that also evolves in x i.e. simulations in which the physics neglected in this article has been included. The profiles used to calculate the theoretical dispersion curves were taken from linear simulations of the experiment of Froula *et al.* for an applied field of 8 T.

Mechanism

The physical causes behind the instability are perhaps best understood by considering each aspect of the positive feedback process in turn. We do this by ignoring all terms on the right hand sides of equations (1) and (2) except for those leading to the Nernst effect (terms in $\beta_{\wedge}$) and Righi-Leduc heat-flow (terms in $\kappa_{\wedge}$), i.e.

$$\frac{\partial B}{\partial t} = \frac{1}{e}\frac{\partial}{\partial y}\left(\beta_{\wedge}\frac{\partial T_e}{\partial y}\right) \tag{19}$$

and

$$\frac{\partial T_e}{\partial t} = \frac{2}{3n_e}\nabla\cdot\left(\frac{\tau_B T_e}{m_e B}\kappa_{\wedge}\mathbf{B}\times\nabla T_e\right). \tag{20}$$

i) The affect of a temperature perturbation on magnetic field

Consider a temperature perturbation of the form $\delta T \sin(ky)$ on top of a bulk profile T_0 (c.f. equation (8)). From equation (19), and by using the earlier results (12) and (13), we find

$$\frac{\partial B}{\partial t} = -\frac{\beta_{\wedge}}{e}k^2\delta T\sin(ky), \tag{21}$$

that is, growth of a magnetic field perturbation in anti-phase with the temperature perturbation. Physically this is a result of the compressional aspect of Nernst advection. The Nernst velocity (the velocity of advection) is proportional to $-\partial T/\partial y$ so that magnetic field is compressed in the troughs of the temperature perturbation and rarefracted at the peaks. Hence we find that a perturbation in the temperature induces one in the magnetic field out of phase by π.

ii) The affect of a magnetic field perturbation on temperature

Now consider a plasma with a temperature profile $\partial T_0/\partial x < 0$ (but with no gradients in the y-direction) subject to a uniform magnetic field on which a perturbation of the form $\delta B\sin(ky)$ has been added (c.f. equation (9)). From equation (20) we find

$$\frac{\partial T_e}{\partial t} = k\frac{2\tau_B T_e}{3n_e m_e}\frac{\partial T_e}{\partial x}\frac{\partial \kappa_\wedge}{\partial \chi}\frac{\chi}{B}\delta B\cos(ky) \qquad (22)$$

so that if $\partial\kappa_\wedge/\partial\chi < 0$ the magnetic field perturbation will induce a temperature perturbation that leads by $\pi/2$. This effect is due to the dependence of $\kappa_\wedge$ on χ, which is itself directly proportional to B (see fig. 4). Since $\partial\kappa_\wedge/\partial\chi < 0$, regions of higher magnetic field strength have a lower Righi-Leduc heat-flow, so that heat is transported away from these regions more slowly than regions of higher B. In this way thermal energy is built up in places where heat-flow goes from high to low (as we move along the positive y-axis) and removed from places where the flow goes from low to high. Notice that if $\partial\kappa_\wedge/\partial\chi > 0$ the reverse is found and a temperature perturbation is generated which lags by $\pi/2$.

The two stages of the feedback process result in induced perturbations which have different phases. Magnetic field perturbations will 'pull' temperature perturbations towards a phase difference of $\pm\pi/2$ (depending on the sign of $\partial\kappa_\wedge/\partial\chi$), while temperature perturbations 'pull' magnetic field perturbations towards a phase of π. The net result of this interaction is that perturbations propagate in the positive y-direction if $\partial\kappa_\wedge/\partial\chi > 0$ or the negative y-direction if $\partial\kappa_\wedge/\partial\chi < 0$, and have a phase difference of $\phi \approx 3\pi/4$ (approximately halfway between π and $\pi/2$).

These more qualitative features are reflected in the stability analysis of §4. Broadly speaking the positive root of (18) can only lead to unstable solutions providing

$$k^3\frac{\partial \kappa_\wedge}{\partial \chi}\frac{\partial T_0}{\partial x} > 0, \qquad (23)$$

(a condition which is necessary but not sufficient). If we take $\partial T_0/\partial x < 0$, this means that $\partial\kappa_\wedge/\partial\chi$ must be negative for waves to grow which propagate in the positive y-direction and *vice versa*.

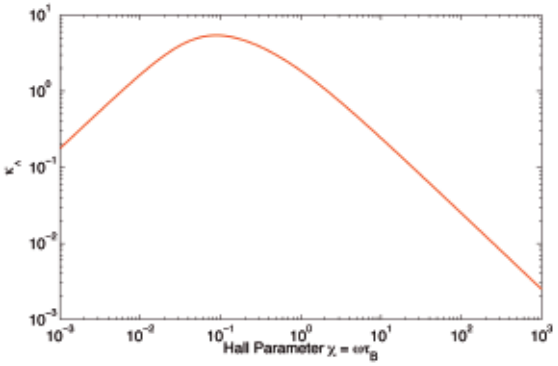

Figure 4. A plot of the variation of $\kappa_\wedge$, the transport coefficient responsible for Righi-Leduc heat flow, with Hall parameter. Notice the maximum value at about $\chi = 10^{-1}$.

More formally, we expect wavelike perturbations to travel with group velocity $v_g = \partial(\Im\{\omega\})/\partial k$. For the x-axis symmetric system discussed above, this means that perturbations either side of $x = 0$ will travel in opposite directions. Notice that the growth rate is unaffected by such a transformation since

$$\omega(x,k) = \omega(-x,-k), \qquad (24)$$

as expected from the symmetry of the problem.

Conclusions and consequences

We have derived the dispersion relation for a previously unknown plasma instability driven by the Nernst effect acting on magnetic fields and the Righi-Leduc heat-flow resulting from bulk temperature gradients. The instability disrupts the uniformity of magnetic field and temperature profiles, leading to periodic lowering of the Hall parameter χ and the subsequent formation of 'islands' of large heat-flow.

We have shown that perturbations obey a relation with growing terms proportional to $k^{3/2}$ and principle diffusive terms (resistive and thermal) that go like k^2. Thus we find unstable behaviour for a range of k up to a cut-off after which diffusive effects become dominant. For parameters similar to those found in the work of Froula *et al.* [1], perturbations with wavelength of order 50 μmn are the fastest growing, having a characteristic growth time of about 0.15 ns – well within the nanosecond timescale of the experiment.

We have also discussed the travelling nature of the instability: perturbations do not grow in a fixed position and instead propagate in a direction which depends on both temperature gradients and the sign of $\partial\kappa_\wedge/\partial\chi$ (and so with Hall parameter $\chi = \omega_e\tau_B$).

The full consequences of the instability are yet to be elucidated, but we can speculate as to its likely affect on the investigation of Froula *et al.* In this case we expect the instability to compromise attempts to suppress non-local heat-flow, which, rather than being reduced by large imposed fields, will instead be squeezed through regions in which the Hall parameter is lowered.

Acknowledgements

This work was supported by the U.K. Engineering and Physical Sciences Research Council.

References

1. D. H. Froula *et al.*, *Phys. Rev. Lett.* **98**, 135001 (2007).
2. A. Raven *et al.*, *Phys. Rev. Lett.* **41**, 8 (1978).
3. P. M. Nilson *et al.*, *Phys. Rev. Lett.* **97**, 255001 (2006).
4. C. K. Li *et al.*, *Phys. Rev. Lett.*, **99**, 055001 (2007).
5. C. K. Li *et al.*, *Phys. Rev. Lett.*, **99**, 015001 (2007).
6. D. H. Froula *et al.*, *Plasma Phys. Control. Fusion.* **51**, 024009 (2009).
7. D. A. Tidman and R.A. Shanny, *Physics of Fluids*, **17**, no.6, p.1207 (1974).
8. A. Hiroa and M. Ogasawara, *Journal of the Physical Society of Japan*, **50**, no.2, p.668 (1981).

9. E. S. Weibel, *Phys. Rev. Lett*. **2**, 83-84 (1959).
10. M. G. Haines, *Journal of Plasma Physics*, **12**, no.1 pp1-14 (1974).
11. M. G. Haines, *Phys. Rev. Lett*. **47**, 917-920 (1981).
12. J. R. Davies *et al*., *Plasma Physics and Controlled Fusion*, **51**, 035013 (2009).
13. C. P. Ridgers *et al*., *Phys. Rev. Lett*. **100**, 075003 (2008).
14. C. P. Ridgers, *Magnetic Fields and Non-Local Transport in Laser Plasmas*, Ph.D. Thesis, Imperial College London (2008).
15. A. Nishigucji *et al*., *Physics of Fluids*, **28**, no.12 p.3683 (1985).
16. S. I. Braginskii in *Reviews of Plasma Physics*. **1**, p.205. (Consultant Bureau, New York, 1966).
17. M. G. Haines, *Plasma Physics and Controlled Fusion*, **28**, no.11, p.1705 (1986).
18. E. M. Epperlein, *J. Phys. D: Appl. Phys*. **17**, pp1823-1827 (1984).
19. E. M. Epperlein and M. G. Haines, *Physics of Fluids*, **29**, no.4, p.1029 (1986).
20. C. P. Ridgers *et al*., *Physics of Plasmas*, **15**, 092311 (2008).